Primljen / Received: 20.10.2023.
Ispravljen / Corrected: 22.5.2024.
Prihvaćen / Accepted: 19.6.2024.
Dostupno online / Available online: 10.7.2024.

Modal deflection method for bridge load testing: a practical alternative to static load tests

Authors:

Shukun Li, MCE
lsk1013705904@163.com

Sheng Qi, MCE
835662566@qq.com

Ruofan Zhao, MCE
1847412121@qq.com

Prof. **Xingjun Qi**
2184099356@qq.com
Corresponding author

Assoc.Prof. **Sanpeng Cao**
1123601978@qq.com

Shandong Jianzhu University
Faculty of Traffic Engineering
Jinan, Shandong, China

Original research paper

Shukun Li, Sheng Qi, Ruofan Zhao, Xingjun Qi, Sanpeng Cao

Modal deflection method for bridge load testing: a practical alternative to static load tests

This study investigated the effectiveness of modal deflection testing as a substitute for static load tests, focusing on the separation of the Ji-Jiao railway separated overpass. The designed load test schemes for both the central and eccentric loading conditions were used to measure the real-time static deflections of the bridge to assess its bearing capacity. Modal testing based on ambient excitation was employed to capture the acceleration vibration responses and identify the key modal parameters of the bridge. The Kriging interpolation method was utilised to extend the mode shapes along both the longitudinal and transverse directions of the bridge deck. The flexibility matrix of the main beam was computed, the modal deflections of the bridge under static test vehicle loads were predicted, and a comparative analysis was conducted using the measured static deflections from the static load test. The results showed that the modal deflections at the midspan section closely matched the static deflections, with errors consistently below 10%. This suggests that modal testing can effectively replace static load tests, providing a viable method for assessing the bridge load-bearing status and enabling real-time health monitoring. This achievement has practical engineering value and opens up prospects for future research.

Key words:
modal test, flexibility matrix, modal deflection, Kriging interpolation method

Izvorni znanstveni rad

Shukun Li, Sheng Qi, Ruofan Zhao, Xingjun Qi, Sanpeng Cao

Metoda modalnog progiba za ispitivanje mosta: praktična alternativa ispitivanju statičkim opterećenjem

U radu je prikazano istraživanje učinkovitosti određivanja modalnog progiba kao zamjene za ispitivanje statičkim opterećenjem, s fokusom na željeznički nadvožnjaka Ji-Jiao. Projektirane sheme simetričnog i nesimetričnog opterećenja upotrijebljene su za mjerenje statičkih progiba mosta u stvarnom vremenu kako bi se procijenila njegova nosivost. Provedena su dinamička ispitivanja s ambijentalnom pobudom kako bi se zabilježilo ubrzanje i odredile modalni parametri mosta. Kriging metoda interpolacije upotrijebljena je za proširenje modalnog oblika u uzdužnom i poprečnom smjeru mosta. Određena je matrica fleksibilnosti glavne grede, predviđeni su modalni progibi mosta pod statičkim opterećenjem vozila i provedena je usporedba s izmjerenim statičkim progibima. Rezultati su pokazali da su modalni progibi na srednjem dijelu raspona dobro usklađeni sa statičkim progibima, s učestalošću pogrešaka nižom od 10 %. To pokazuje da dinamičko ispitivanje može učinkovito zamijeniti ispitivanja statičkim opterećenjem, pružajući održivu metodu za procjenu stanja nosivosti mosta, omogućavajući praćenje u stvarnom vremenu. Ovo postignuće ima praktičnu vrijednost i otvara prilike za buduća istraživanja.

Ključne riječi:
dinamičko ispitivanje, matrica fleksibilnosti pomaka, modalni progib, Krigingova metoda interpolacije

1. Introduction

Bridges serve as crucial and central facilities that facilitate interconnection and communication between transportation systems. The safety, usability, and durability of these structures have consistently been the focal points of civil engineering research. Throughout the life cycle of bridge structures, the cumulative impacts of factors such as material ageing, environmental erosion, long-term load effects, fatigue, and severe vehicle overloading inevitably result in structural damage. This damage significantly diminishes the load-bearing capacity of the bridge, posing a significant threat to its safe operation [1-4]. An accurate and scientific assessment of the structural bearing conditions of in-service bridges is essential to ascertaining their actual safety margins, thereby effectively mitigating potential catastrophic consequences during operational phases.

Traditional methods for assessing the load-bearing state of bridges include the load test method, synthetic evaluation approach, and influence line method [5-9]. Among them, the load testing method is the most accurate and objective approach and plays a crucial role in the safe maintenance of bridges. However, owing to the large-scale and lengthy traffic control required for static load tests, their economic feasibility is relatively poor. Therefore, conducting systematic assessments of the load-bearing capacities of numerous small- to medium-sized bridges on a large scale is unsuitable. With ongoing technological advancements in computing and data acquisition systems, the application of advanced sensors and structural dynamic testing for condition assessment has seen significant developments in recent years [10].

In practical bridge dynamic testing, particularly when the ambient excitation is considered, only the fundamental modal parameters of a bridge can be obtained [11]. Accurately evaluating the bearing capacity of bridge structures is challenging when relying solely on these fundamental modal parameters. The utilisation of modal parameters, particularly the modal flexibility of bridge structures, has emerged as a focal point in global research. Zhou et al. [12, 13] introduced a substructure modal shape splicing method to calculate the flexibility matrix of a structure, thereby enhancing the efficiency of modal testing using the multireference point pulse hammer method. Tian et al. [14, 15] conducted multireference impact and static tests on long-span bridges and demonstrated good agreement between the predicted and calculated deflections. Qi et al. [16] applied an additional mass method to obtain the modal deflection of a bridge and used it to assess the actual bearing capacity of a simply supported hollow slab bridge and a continuous beam bridge based on ambient excitation and bridge load test results.

In practical engineering applications, owing to the constraints stemming from testing method, experimental equipment, and testing conditions, the assessment method for the load-bearing capacity of real bridges still requires continuous expansion and refinement. This study introduces a method for evaluating the load-carrying capacity of bridges based on non-interrupted traffic using modal deflection testing. The effectiveness and feasibility of the proposed method were validated through static and dynamic tests on an assembled, simply supported T-beam bridge at a separated-grade junction on the Ji-jiao Railway. This method does not require prolonged traffic interruptions or the utilisation of traffic gaps for bridge testing and is both convenient and efficient, offering significant practical engineering value for a multitude of small- and medium-sized highways and urban bridges.

2. Theoretical background

The mode shape reflects the inherent characteristic of the structure and represents the ratio of the modal deflection of the structure in different modal orders. According to the orthogonality of the mode shapes [17, 18]:

$$\begin{aligned} \text{diag}(M_i) &= \varphi^T M \varphi \\ \text{diag}(C_i) &= \varphi^T C \varphi \\ \text{diag}(K_i) &= \varphi^T K \varphi \end{aligned} \quad (1)$$

where M denotes the mass matrix, C is the damping matrix, and K is the stiffness matrix. φ is the displacement mode matrix, $\varphi = \varphi_1\varphi_2\varphi_3 \ldots \varphi_i$, and φ_i is the corresponding ith mode shape vector. Eq. (1) shows that the identified arbitrary displacement mode φ_i of the structure satisfies the orthogonality condition. The mass and stiffness matrices of the structure can be diagonalised, as shown in Eqs. (2) or (3):

$$\begin{aligned} \varphi^T M \varphi &= \text{diag}(m_i) \\ \varphi^T K \varphi &= \text{diag}(k_i) \end{aligned} \quad (2)$$

$$\begin{aligned} \varphi^T M \varphi &= m_i \\ \varphi^T K \varphi &= k_i \end{aligned} \quad (3)$$

where: i = 1, 2, 3, 4 .... n

For the i-th mode, when there exists a displacement mode $\overline{\varphi}_i$ that satisfies $\overline{\varphi}_i^T M \overline{\varphi}_i = m_i = 1$, $\overline{\varphi}_i$ is referred to as the mass-normalised displacement mode, and the corresponding mode shape matrix $\overline{\varphi}$ is the mass-normalised displacement mode shape matrix.

The mass matrix of a structure is certain, and its corresponding mass-normalised displacement mode shape for a certain mode is determined. The displacement mode φ_i obtained from the modal eigenvalue analysis or modal analysis identification may not necessarily be the exact mass-normalised displacement mode shape. A proportional coefficient a_i exists between this and the corresponding mass-normalised displacement mode shape $\overline{\varphi}_i$, as shown in Eq. (4):

$$\overline{\varphi}_i = \frac{\varphi_i}{a_i} \quad (4)$$

Substitute Eq. (4) into $\overline{\varphi}_i^T M \overline{\varphi}_i = 1$ to get the proportional coefficient a_i.

$$a_i = \sqrt{\varphi_i^T M \varphi_i} \quad (5)$$

By substituting the mass-normalised displacement mode shapes matrix into Eq. (2):

$$\bar{\varphi}^T M \bar{\varphi} = \text{diag}(\bar{m}_i) = I$$
$$\bar{\varphi}^T K \bar{\varphi} = \text{diag}(\bar{k}_i) = I \quad (6)$$

In the case that $\bar{\varphi}$ is a square matrix with full rank, for both sides of the second Eq. (6), multiply $(\bar{\varphi}^T)^{-1}$ by left and $(\bar{\varphi})^{-1}$ by right simultaneously to obtain the stiffness matrix of the structure as follows:

$$K = \left(\bar{\varphi}^T\right)^{-1} diag(\bar{k}_i)(\bar{\varphi})^{-1} \quad (7)$$

The flexibility matrix F^d of the structure is the inverse of the stiffness matrix K, as shown in Eq. (8):

$$F^d = K^{-1} = \bar{\varphi} diag\left(\frac{1}{\bar{k}_i}\right)\bar{\varphi}^T = \sum_{i=1}^{n} \frac{\bar{\varphi}_i \bar{\varphi}_i^T}{\bar{k}_i} \quad (8)$$

where d indicates that this parameter belongs to displacement. The relationships among the natural frequency w_i, modal mass $\bar{m}_i$ and modal stiffness $\bar{k}_i$ are as follows:

$$w_i = \sqrt{\frac{\bar{k}_i}{\bar{m}_i}} \quad (9)$$

The modal mass $\bar{m}_i = 1$ corresponding to the mass-normalised mode shape $\bar{\varphi}_i$ is equal. Therefore,

$$\bar{k}_i = w_i^2 \quad (10)$$

Substituting these values into Eq. (8) yields the following formula for calculating the flexibility matrix:

$$F^d = \sum_{i=1}^{n} \frac{\bar{\varphi}_i \bar{\varphi}_i^T}{w_i^2} \quad (11)$$

Where $\bar{\varphi}_i$ is the ith order mass-normalised mode shape, w_i^2 is the ith order natural frequency, and *n* is the total number of identified modes.
Finally, the flexibility matrix is calculated using Eq. (11) can be substituted into Eq. (12) to obtain the modal deflection.

$$\Delta = F^d f \quad (12)$$

where Δ is the modal deflection and f is the static load vector.

3. Field test

3.1. Project overview

The Ji-jiao railway separated overpass is a dual-carriageway bridge that allows bidirectional travel, with a bridge span combination of 25 m + 30 m + 25 m. Each carriageway consists of seven precast prestressed concrete simply supported T-beams laterally. The substructure was composed of column piers, gravity-type U-shaped abutments, and bored pile foundations. A simply supported T-beam bridge span of 25 m was selected as the experimental subject. The bridge is illustrated in Figure 1, and its dimensions are shown in Figure 2.

Figure 1. Studied bridge

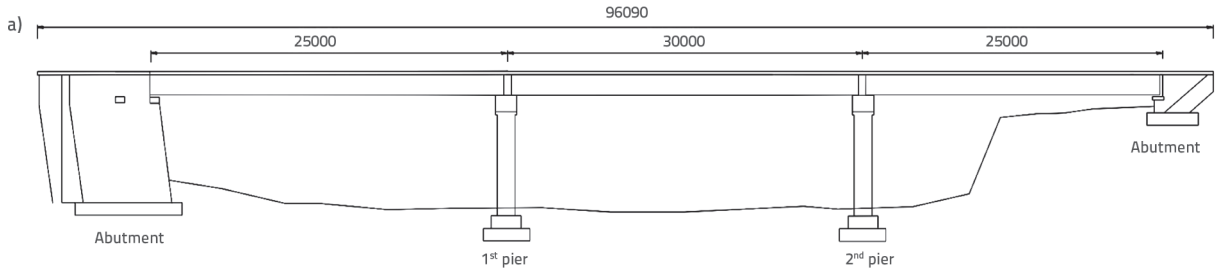

Figure 2. Bridge dimensions (mm): a) Longitudinal view of the bridge

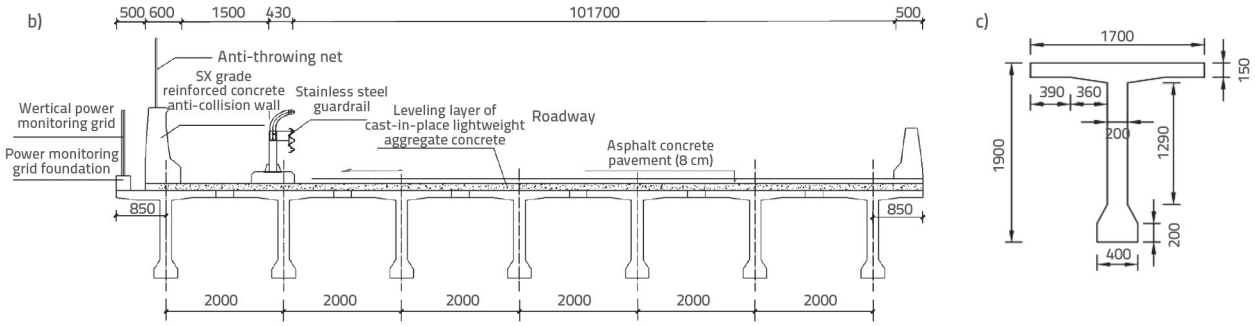

Figure 2. Bridge dimensions (mm): b) Bridge cross-section; c) Beam cross-section

3.2. Bridge finite element model

To accurately correlate the theoretical modeshapes of the bridge with the identified mode shapes, determine the minimum order required to capture the predicted modal deflections, and extract the mass matrix from the finite element model, finite element modelling of the bridge must be conducted. The finite element software ANSYS was used to establish a bridge model. Owing to the large width of the bridge deck, a single-beam model could not accurately simulate the lateral response of the bridge structure under an experimental load. Therefore, this study adopted a beam grid model for the finite element simulation. The main beam, virtual transverse beam, solid transverse beam, and guardrail were modelled using BEAM4 elements. The concrete levelling layer was represented by SHELL63 elements. The asphalt layer was simplified as a concentrated mass and integrated into the bridge body, with COMBIN14 elements employed to simulate the vertical support action of all beam-end bearings. The main beam, solid transverse beam, and guardrail have an elastic modulus of 1.55×10^4 MPa, a density of 2500 kg/m^3, a Poisson's ratio of 0.2, and the element length of the finite element model is 0.4 m. The virtual transverse beam has a density of 0 kg/m^3. The elastic modulus of the concrete levelling layer is 3.25×10^4 MPa, with a density of 2500 kg/m^3 and Poisson's ratio of 0.2, and the thickness of the concrete levelling layer is 0.08 m. Because of the small ratio of the steel reinforcement area to the main beam area in the main beam section and the bridge being in an elastic state, no steel reinforcement elements were established in the constructed bridge models. The finite element model of the bridge is depicted in Figure 3, and the first four theoretical modal shapes are illustrated in Figure 4.

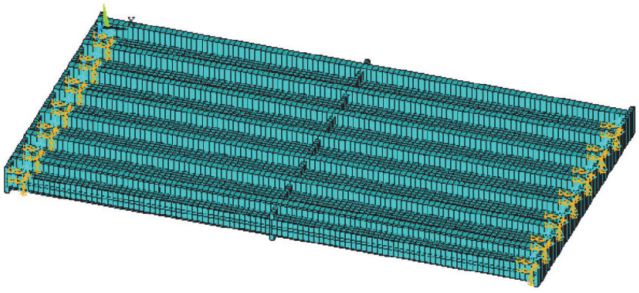

Figure 3. Finite element model of the bridge

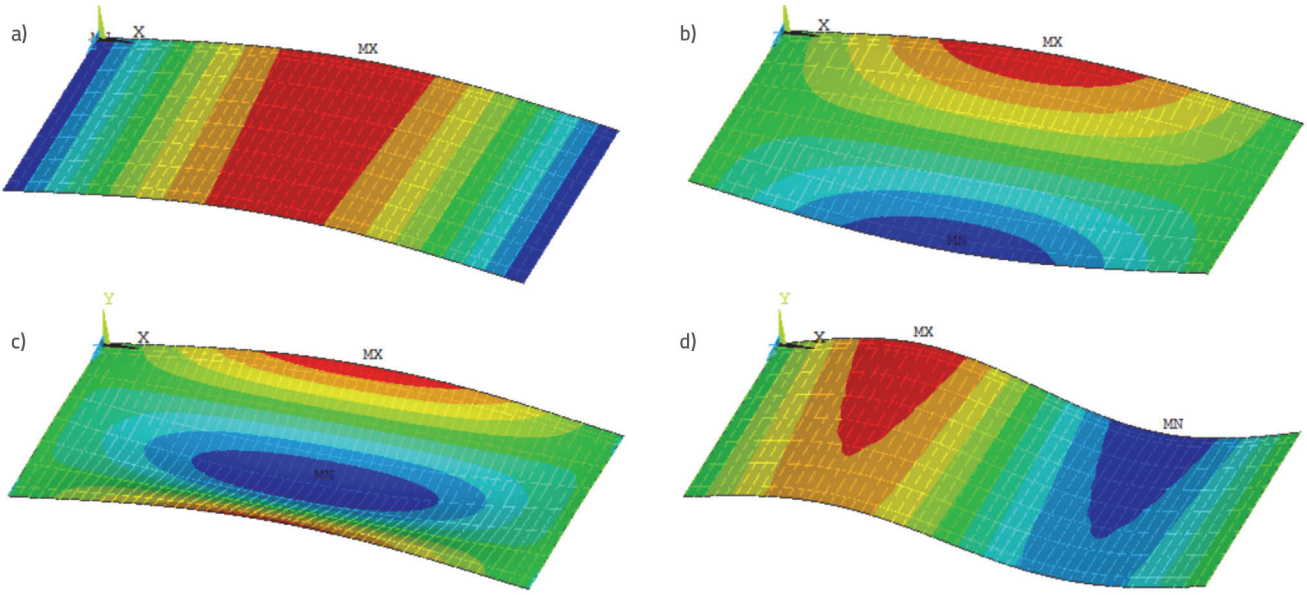

Figure 4. First four theoretical modal shapes: a) First modal shape; b) Second modal shape; c) Third modal shape; d) Fourth modal shape

4. Static load test

Before performing a static load test on a bridge, the loading efficiency of the test must be calculated in accordance with the *Load Test Methods for Highway Bridges* (JTG/T J21-01—2015) [19]. This calculation is essential to fully elucidating the structural characteristics under an applied load. The loading efficiency (η_q) was determined using Eq. (13).

$$\eta_q = \frac{S_s}{S(1+\mu)} \tag{13}$$

where S_s refers to the maximum calculated effect value of internal forces or displacements within the loading section for a specific loading test project under a static loading test load, S represents the most adverse calculated value of internal forces or displacements within the loading section generated by the load, and μ represents the shock coefficient value. The impact coefficient of automobiles varies between 0.05 and 0.45, depending on the fundamental frequency of the structure. According to [19],the impact coefficient is calculated as follows:

when $f < 1{,}5$ Hz, $\mu = 0.17671 \cdot \ln f - 0.0157$ (a)
when $1{,}5\ \text{Hz} \le f \le 14$ Hz, $\mu = 0.17671 \cdot \ln f - 0.0157$ (b)
when $f > 14$ Hz, $\mu = 0.45$ (c)

The theoretical calculation yielded a fundamental bridge frequency of 4.433 Hz; therefore, condition (b) was selected for the calculation.

To ensure the accuracy of the test results, it is imperative to adhere to the specifications outlined in the *Specification for Inspection and Evaluation of Load-bearing Capacity of Highway Bridges* (JTG/T J21—2011) [20]. According to this code, the loading efficiency of a bridge should ideally range between 0.95 and 1.05. Four three-axle load vehicles were used for this purpose: a front axle load of 76 kN, a middle axle load of 148 kN, and a rear axle load of 148 kN. The arrangement of the loading vehicles on site is shown in Figure 5. A schematic depicting the dimensions of the loaded vehicles is shown in Figure 6.

The static load test of the Ji-jiao railway separated overpass was divided into two loading conditions: the central and eccentric load conditions. To verify the proper functioning of the testing system and the organisation of the experiment, the preloading holding time should not be less than 20 min, during which

Figure 5. Phase of static testing of the bridge with 4 trucks

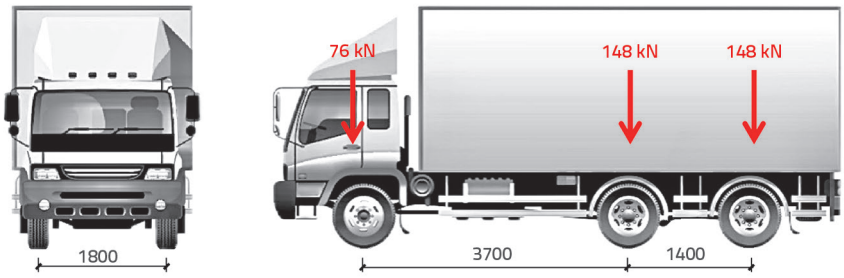

Figure 6. Schematic of the loading vehicle dimensions (mm) and axle load [kN]

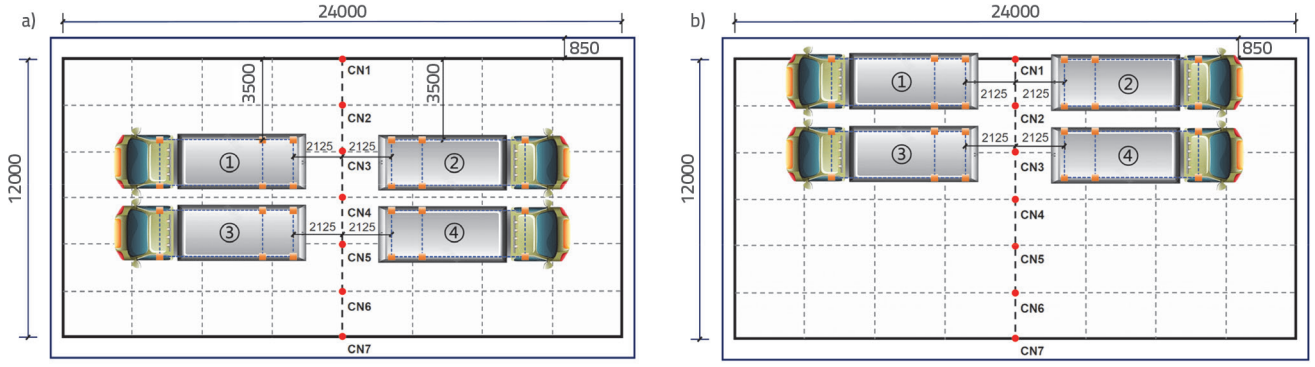

Figure 7. Load test conditions: a) Central load condition [mm]**; b) Eccentric load condition** [mm] **(First-level loading condition:** ①+②**, Second-level loading condition:** ①+②+③+④)

the load is gradually reduced to zero and the structure has sufficient time to recover to zero load. Once the structure has fully recovered to zero load, the formal loading can commence.

The test employed a step-by-step loading approach, and all procedures were conducted using a two-step loading method. The first-level loading condition involves Vehicles ① and ②, while the second-level loading condition involves Vehicles ①,②,③, and ④. The locations of the loading vehicles are shown in Figure 7.

Each loading procedure and reading should be measured immediately after loading or unloading, and stable readings should be taken after the loading or unloading has stabilised. A sign of relative stability in the structure is when, within the last 5 min of each load level, the incremental displacement is less than 15 % of the incremental displacement within the preceding 5 min or less than the minimum resolution of the measuring instrument used. The readings taken after stabilising the first-level loading condition are referred to as the first-level stable deflections, whereas those taken after stabilising the second-level loading condition are referred to as the second-level stable deflections. Because the midspan is the most critical location on a bridge, each midspan of the main beam was chosen as the measurement point. The measurement points were designated as CN1–CN7. The layout of the measurement points is shown in Figure 8. Supports were installed underneath the bridge to secure the TST-100A displacement sensors (sensitivity: 48,60 με/mm). Bridge deflection data were collected using a data acquisition system. The onsite test setup is shown in Figure 9. The recorded deflection values at the mid-span section of the main beam of the bridge under central and eccentric load conditions are presented in Tables 1 and 2, respectively.

Observation of the data in the table indicates that under both central and eccentric loading conditions, the relative residual deformation of the measurement points after unloading was significantly less than 20 %, meeting the requirements of the *Technical Code for Test and Evaluation of City Bridges* (CJJ/T 233-2015) [21]. The elastic working states of the rehabilitated and reinforced bridges were satisfactory.

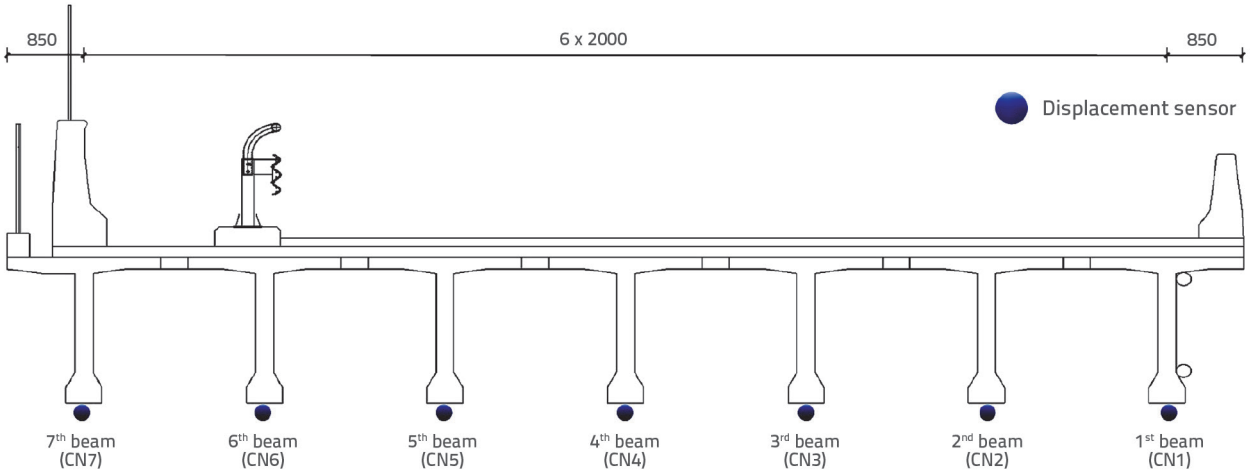

Figure 8. Layout of the deflection measurement points

Figure 9. Setup for deflection measurement under the bridge: a) Setup method of displacement sensor; b) Layout of data acquisition system

Table 1. Deflection value for the central load control sections

Number	First-level stable deflection [mm]	Second-level stable deflection [mm]	Unloading deflection [mm]	Elastic deformation [mm]	Relative residual deformation [%]
CN1	-0.25	-1.08	0.04	-1.12	3.70
CN2	-0.73	-2.07	-0.04	-2.03	1.93
CN3	-1.09	-2.73	-0.04	-2.69	1.47
CN4	-1.41	-3.06	-0.04	-3.02	1.31
CN5	-1.70	-2.98	-0.16	-2.82	5.37
CN6	-1.43	-2.17	-0.02	-2.15	0.92
CN7	-1.13	-1.49	0.00	-1.49	0.00
Note: CN1–CN7 are control points corresponding to the mid-span of the seven main beams.					

Table 2. Deflection values for the eccentric load control sections

Number	First-level stable deflection [mm]	Second-level stable deflection [mm]	Unloading deflection [mm]	Elastic deformation [mm]	Relative residual deformation [%]
CN1	-1.52	-2.38	0.00	-2.38	0.00
CN2	-1.34	-2.74	0.00	-2.74	0.00
CN3	-1.15	-2.81	0.00	-2.81	0.00
CN4	-0.71	-2.27	0.00	-2.27	0.00
CN5	-0.49	-1.68	-0.02	-1.66	2.67
CN6	-0.02	-0.75	-0.02	-0.73	1.19
CN7	0.00	-0.36	0.00	-0.36	0.00
Note: CN1–CN7 are control points corresponding to the mid-span of the seven main beams					

5. Modal testing of interchange bridge

5.1. Modal testing

With the enhanced sensitivity of sensors and progress in internet technology, the environmental vibration test method has become widespread in bridge modal testing. This method relies on ambient excitations, such as ground motion, wind load, and vehicle load, to induce bridge vibrations. The vibration response of a bridge can be recorded using high-sensitivity vibration sensors, data acquisition systems, and computers. Modal analysis methods such as peak picking, empirical mode decomposition, and the random subspace method [22, 23] are then employed to identify the modal parameters of the bridge structure.

Comparing this ambient excitation method with the traditional approach, which simultaneously uses input and output information to identify bridge modal parameters, offers several advantages. First, it eliminates the need to measure the structure's excitation information and directly identifies the modal parameters using the vibration response data, thereby reducing the workload and enhancing practicality. Second, the environmental vibration testing method does not require interruption of the normal operation of bridge structures, whereas traditional manual excitation requires complex excitation equipment, which is expensive, and the excitation process requires traffic control, making it less suitable for bridges with heavy traffic flow.

The modal test described in this study adopts the ambient random excitation testing method. The BY-S07 accelerometer sensors (sensitivity: 0,3 v/(m/s^2) were strategically positioned at eight equidistant points on each main beam. An appropriate amount of organic mud was evenly spread into thin sheets and adhered to the bottom of the accelerometer. Tight adhesion between the mud and the bottom of the sensor securely fastens the accelerometer with mud to the bridge deck, ensuring that the sensor remains stable during testing. A single-point moving test technique was used by fixing one accelerometer at a measuring point, referred to as the reference point, and moving the other sensor points in three batches to collect data. This is combined with the modal synthesis technique to obtain full-bridge modal information. To fully capture the vibration response of the bridge structure, the sampling time for each batch was set to 20–30 min with a sampling frequency of 500 Hz. The on-site bridge testing is depicted in Figure 10, and the layout of the measurement points is illustrated in Figure 11.

Figure 10. Field photograph of the modal test

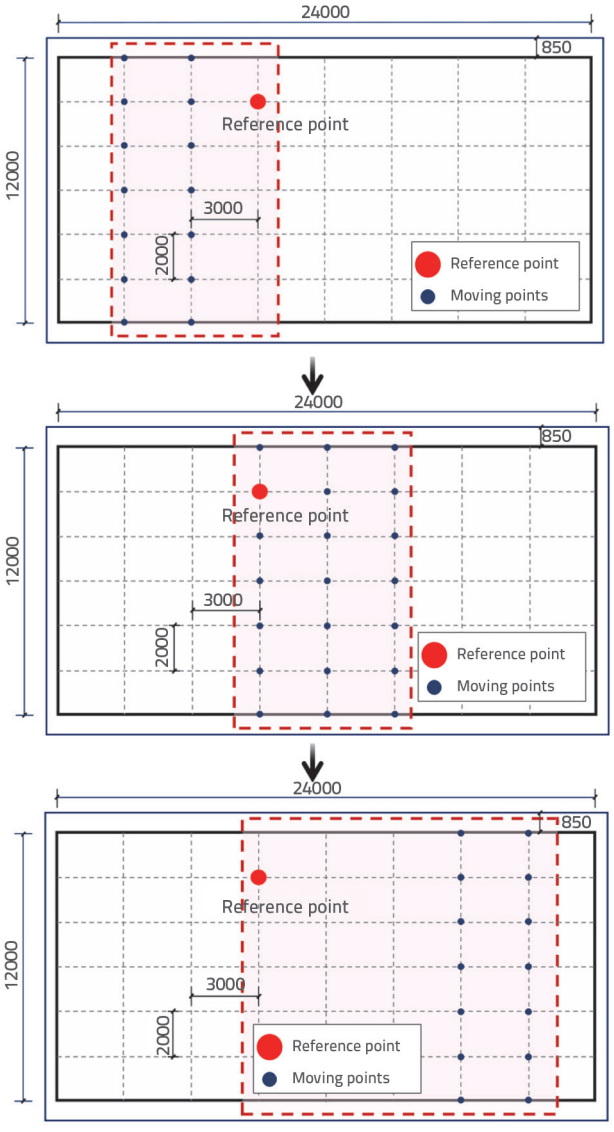

Figure 11. Layout of the measurement points (dimensions in mm)

5.2. Bridge modal parameter identification

When assessing the load-carrying capacity state of bridges using the ambient excitation-based modal deflection testing method, the displacement flexibility matrix exhibited rapid modal convergence. Consequently, the higher-order modal parameters contribute only minimally to the displacement flexibility matrix. Thus, only modal parameters of the first few orders are typically required to obtain a sufficiently accurate displacement flexibility matrix [24].

By identifying the displacement flexibility matrix, the modal deflection of the bridge was predicted, and the predicted results quickly converged to the actual static deflection of the structure. Consequently, for this simply supported beam bridge, it is only necessary to identify the modal parameters of the first four modes for predicting the deflections at the midspan control section to satisfy the precision requirements. The modal parameters of the simply supported T-beam bridge were identified using the SSI modal identification method. The frequency identification results are listed in Table 3.

During the bridge construction process, to ensure bridge stability, a certain safety margin was incorporated, resulting in a higher stiffness K, which caused the measured identification frequency to be greater than the theoretical frequency. The first four modal shapes of the bridge are shown in Figure 12.

When the modal test point layout does not coincide with the positions of wheel loading during static load tests, failure to conduct load distribution leads to a mismatch between the displacement flexibility matrix acquired from modal testing and the load vector from static load testing. There are significant errors in the modal deflections calculated using Eq. (11) compared with the static deflections measured from the static load tests. Distributing the wheel loads to nearby measurement points and considering only the vertical load distribution failed to accurately reflect the effects of the loaded wheels on the bridge structure.

The modal shapes identified from the modal testing at 49 measurement points were subjected to interpolation processing in both the transverse and longitudinal directions of the bridge. Using this method, the mode shape data at the wheel load application points can be obtained, allowing the calculation of the displacement flexibility matrix corresponding to the actual wheel load vector. This process facilitates the prediction of modal deflections and eliminates the need for a specific wheel-load distribution.

Common interpolation methods include inverse distance interpolation, radial basis functions, and kriging interpolation [25-27]. Compared to traditional modal extrapolation methods,

Table 3. Frequency identification results

Modal order	First mode of the first modal shape	Second mode of the second modal shape	Third mode of the third modal shape	Fourth mode of the fourth modal shape
Theoretic frequency [Hz]	4.433	6.988	12.959	17.748
Identification frequency [Hz]	6.475	7.575	13.381	20.581

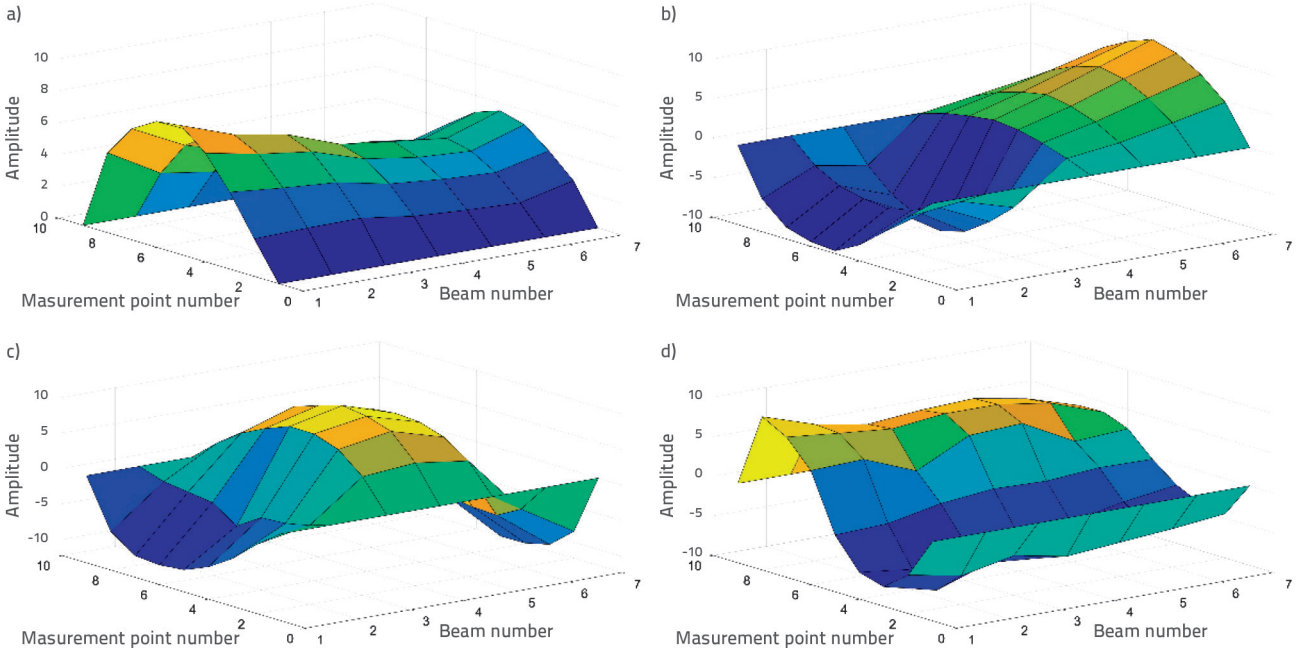

Figure 12. Identification results for the first four modal shapes: a) First modal shape; b) Second modal shape; c) Third modal shape; d) Fourth modal shape

Table 4. Identification of Modal Assurance Criterion (MAC) values

Load condition	First mode of the first modal shape	Second mode of the second modal shape	Third mode of the third modal shape	Fourth mode of the fourth modal shape
Central load	0.9947	0.8578	0.8887	0.9480
Eccentric load	0.9930	0.8608	0.8623	0.9395

Kriging interpolation imposes fewer restrictions and exhibits wider applicability. It fully considers the spatial correlation of variables, reflects the spatial structure of the variables, and provides a minimum variance estimation of unknown data within the estimation area, thus demonstrating excellent smoothing effects. These advantages give the Kriging method superior simulation performance compared to other common interpolation methods.

Therefore, this study utilised the Kriging method to interpolate and extend the measured mode shapes. During modal testing, the measurement points were positioned at every eighth point along each beam. Virtual measurement points were introduced at the wheel locations, and the mode shape values at these virtual points were obtained by interpolation using the actual measurement point values. The extended modal shapes for the first four modes of the bridge after interpolation are illustrated in Figure 13, and the determination of Modal Assurance Criterion (MAC) values is presented in Table 4.

The MAC is used to assess the correlation of modal vibration vectors in the modal space. The computed scalar value falls between zero and one, with a value closer to one indicating a better modal correlation. From Table 4, it is evident that under both central and eccentric load conditions, the MAC value of the extended modes of vibration ranges from 0.85 to 0.99. Notably, the accuracies of the first and second vertical modes of vibration exceeded 0.85, indicating the highest precision among all modes of vibration. The results underscore the reliability of using Kriging to interpolate the modes of vibration at the wheel positions, effectively addressing the challenge of misalignment between the mode-shape measurement points and the loading points.

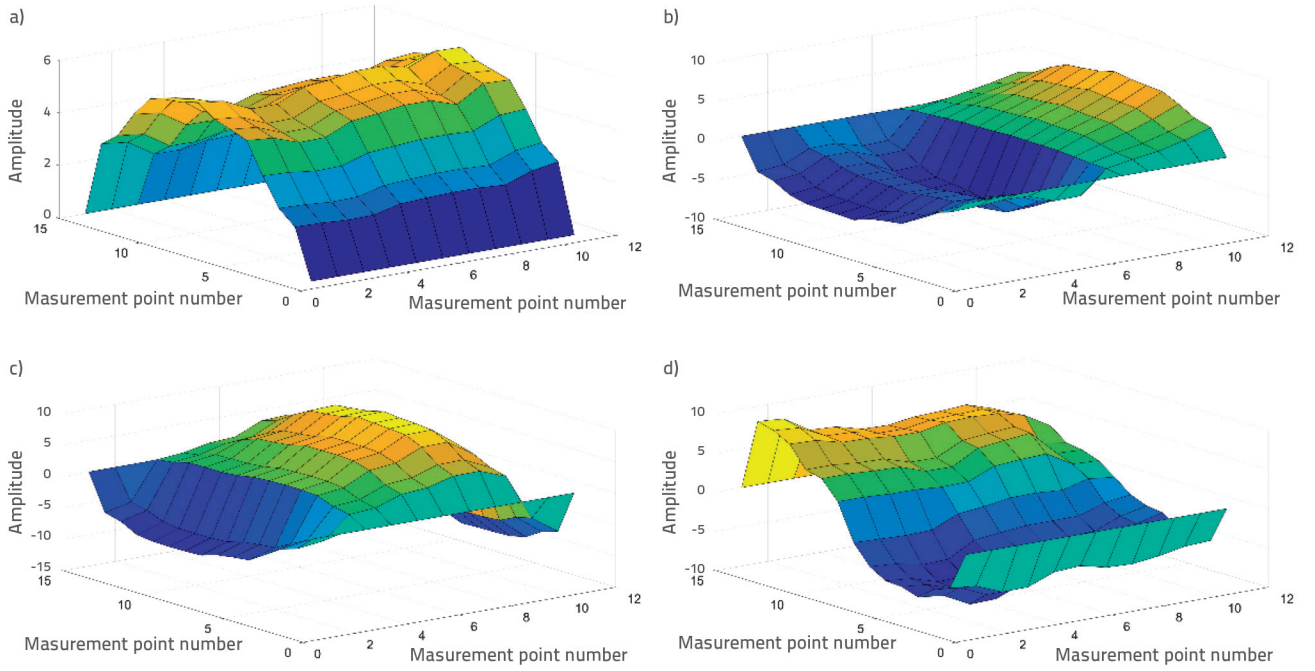

Figure 13. Extended modal shapes for the first four bridge modes after interpolation: a) First modal shape; b) Second modal shape; c) Third modal shape; d) Fourth modal shape

5.3. Displacement flexibility matrix

Flexibility represents the displacement of a structure under a unit force, which is the reciprocal of stiffness, and can characterise the deformation ability of a structure in its elastic state [28, 29]. The element in the displacement flexibility matrix represents the deflection at the node caused by the application of a unit force at the node. A flexibility matrix is used to predict the deflection of a bridge under a known load.

In this study, a refined finite element model was used to normalise the experimental modal shapes, and the normalised modal parameters were used to calculate the flexibility matrix. The first four modal shapes of the bridge were normalised and substituted into Eq. (11) to obtain the displacement flexibility matrix, as follows: To observe the flexibility matrix of the bridge, a three-dimensional plot was drawn, as shown in Figure 14.

The three-dimensional graph of the flexibility matrix evidently shows that it essentially reflects the deformation of the structure under loading. The peak points in the graph correspond to the midspan sections of the bridge edge beam. This result aligns with the physical significance of the overall vertical deformation of the simply supported beam bridge structure.

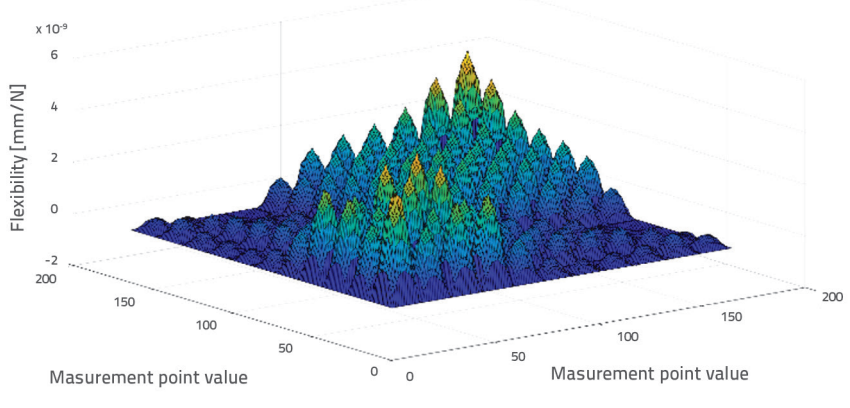

Figure 14. 3D diagram of the compliance matrix

6. Bridge bearing capacity evaluation

Displacement is one of the most critical parameters in structural design or evaluation assessment because it provides an intuitive reflection of the basic performance and stiffness state of a structure. Consequently, the displacement of bridge structures has consistently been the focus of engineers and researchers. Traditionally, the vertical displacement measured directly during a static load test serves as the primary criterion for evaluating the bearing capacity of a bridge. However, owing to the cost implications and time-intensive nature of static load tests, this method is inconvenient for assessing the bearing capacities of numerous small- and medium-sized bridges. The modal deflection of structures under static loading was predicted by utilising the inherent property of the displacement flexibility of bridges. This approach clearly replaces the measured static deflection for the assessment of the

Table 5. Error between the modal and measured static deflections

Number	Central load condition			Eccentric load condition		
	Static deflection [mm]	Modal deflection [mm]	Relative error [%]	Static deflection [mm]	Modal deflection [mm]	Relative error [%]
CN1	-1.12	-1.37	22.3	-2.38	-2.47	4.0
CN2	-2.03	-2.15	6.0	-2.74	-3.00	9.5
CN3	-2.69	-2.61	3.0	-2.81	-2.54	9.7
CN4	-3.02	-2.85	5.8	-2.27	-2.11	6.9
CN5	-2.82	-2.57	8.9	-1.66	-1.51	9.0
CN6	-2.15	-2.08	3.1	-0.73	-0.94	28.8
CN7	-1.49	-1.81	21.5	-0.36	-0.45	25.0
Note: CN1–CN7 are control points corresponding to the mid-span of the seven main beams						

Table 6. Deflection verification coefficient

Number	Central load condition			Eccentric load condition		
	S_s [mm]	S_e [mm]	η	S_s [mm]	S_e [mm]	η
CN1	/	/	/	-3.45	-2.47	0.716
CN2	-4.26	-2.15	0.505	-4.26	-3.00	0.704
CN 3	-4.98	-2.61	0.524	-4.98	-2.54	0.510
CN 4	-5.32	-2.85	0.536	-5.32	-2.11	0.397
CN 5	-4.98	-2.57	0.516	-4.98	-1.51	0.303
CN 6	-4.27	-2.08	0.487	/	/	/
CN 7	/	/	/	/	/	/
Note: CN1–CN7 are control points corresponding to the mid-span of the seven main beams						

bridge carrying capacity, thereby effectively compensating for the shortcomings of traditional static loading tests.

In this study, the displacement flexibility matrix of the Ji-jiao railway separated overpass, combined with the load vector corresponding to the loaded wheel in the static load test, was used to calculate the modal deflection for both the central and eccentric loads in the static load test. The calculated modal deflections were then compared with the measured static deflections obtained from the static load test for error analysis, and the results are presented in Table 5.

According to the data in the observation table, under central load conditions, the deflection values of the beams corresponding to CN2 to CN6 are greater than those corresponding to CN1 and CN7, with an overall relative error of less than 9 % for these five beams. The maximum and minimum relative errors are 8.9 % and 3.0 %, respectively. Under eccentric load conditions, the deflection values of the beams corresponding to CN1–CN5 were greater than those corresponding to CN6 and CN7, with an overall relative error of less than 10 % for these five beams. The maximum and minimum relative errors are 9.7 % and 4.0 %, respectively. The analysis indicated that despite certain deflection differences, the overall relative errors remained at relatively low levels, within 8.9 % and 10 %, respectively. The source of the error is attributed to the truncation of the modal orders; thus, the predicted modal deflections under both loading conditions met the engineering accuracy requirements.

Additionally, for the beams corresponding to CN1 and CN7 under the central load condition and the beams corresponding to CN6 and CN7 under the eccentric load conditions, the measurement points were far from the loading points, resulting in small measured deflection values. Moreover, inherent measurement errors exist in static deflection measurement values. Consequently, the relative errors between the modal and measured deflections are large for these four measurement points. However, beams with smaller measured deflection values had no impact on the assessment of the load-bearing capacity of the bridge.

The deflection verification coefficient η of each main beam was calculated according to [19], and η was calculated according to Eq. (14).

$$\eta = \frac{S_e}{S_s} \tag{14}$$

where η represents the deflection verification coefficient, S_e represents the measured elastic displacement values of the main measuring points under the modal test load,and S_s is the same as in Eq. (13).

After accurately predicting the measured modal deflection of the section at the midspan of the main beam, the modal deflection verification coefficient of the section was calculated. This calculation involved using the predicted modal deflection of the actual bridge under central and eccentric load conditions while eliminating irrelevant measurement points. The calculation results are listed in Table 6.

The results in the table indicate that under central load or eccentric load conditions during load tests, the verification coefficients of deflection calculated using the predicted modal deflections obtained from actual bridge modal testing were all less than 1 for the mid-span section of the Ji-jiao railway separated overpass. This satisfies the specification [19], demonstrating that modal deflection testing based on ambient excitation can effectively assess the load-bearing capacity states of bridges. Furthermore, it is feasible to conduct modal testing on actual bridges without interrupting the traffic flow, indicating significant practical engineering applicability.

7. Conclusion

Given the challenges associated with measuring bridge deflections and the distinctive nature of modal test methods, this study investigated the deflection measurement, identification, and prediction of simply supported T-beam bridges. The findings are summarised as follows:

- Based on the ambient excitation modal testing method, the first four modal parameters of the 49 measurement points on an assembled, simply supported beam bridge were identified. The Kriging interpolation method was used to extend the mode shapes longitudinally and transversely on the bridge deck. The modal deflections in the mid-span section under the static load test were calculated. Compared to the measured static deflections under the central load condition, the maximum relative errors for the five beams with the largest effects were all below 10 %. Similarly, under the eccentric load condition, the maximum relative errors of the five beams with the largest effects were less than 10 %. This essentially meets the engineering accuracy requirements, indicating the high accuracy of the modal deflection prediction based on the ambient excitation modal testing method. It can effectively replace measured static deflections to evaluate the load-bearing capacity of a bridge.
- Using a modal test method to predict the modal deflections of a bridge under various load conditions in a static load test plan and calculating the deflection verification coefficient, combined with the current specification [19], the stiffness of existing bridges can be assessed. Therefore, the bridge ambient excitation modal test method can replace traditional static load tests for bridge load-carrying capacity evaluation.
- The modal deflection test method based on ambient excitation combines the advantages of traditional static and dynamic load tests for evaluating the load-carrying capacity of bridges. It can collect the vibration information of operational bridges without interrupting traffic and facilitate the quick identification of the modal parameters of bridge structures. With the rapid development of testing technologies and modal identification methods, the accuracy of this method continues to improve. Therefore, they have good practical engineering value and broad application prospects.

Acknowledgements

This research was supported by the Shandong Province Housing and Urban Rural Construction Science and Technology Plan Project (No. 2024KYKF-CSGX024), the Science and Technology Plan Project of Jiqing High speed Railway Co., Ltd. (No. JQKJ2024-10), the Science and Technology Plan Project of Shandong Provincial Department of Transportation (No. 2022B06) and the Shandong Province Enterprise Technology Innovation Project (Nos. 202250101726 and 202160101415).

REFERENCES

[1] Xiang, L.: Detection and bearing capacity evaluation of existing concrete bridges, Southwest Jiaotong University, 2017.

[2] Yi-feng, Z., Jin-song, Z.: Damage identification for bridge structures based on correlation of the bridge dynamic responses under vehicle load, Structures, 33 (2021), pp. 68-76

[3] Yu-zhao, L., Feng, X.: Measurement-based bearing capacity evaluation for small and medium span bridges, Measurement, 149 (2020).

[4] Fang, Z., Kai-quan, Z., Jie-chao, D., Qian, Y., Xiang, W., et al.: Research progress of bridge evaluation and reinforcement in 2020, Journal of Civil and Environmental Engineering, 43 (2021), pp. 152-166.

[5] Chuang, L., Su-feng, Z.: Research on rapid detection and identification method of bridge structure, Highway Traffic Technology, 6 (2004), pp. 60- 65, 85

[6] Dong-ping, L., Xin-kui, T., Ning-bo, W.: Bridge rapid detection method based on actual influence line, Bridge construction, 49 (2019), pp. 42-46

[7] Sasmal, S., Ramanjaneyulu, K.: Condition evaluation of existing reinforced concrete bridges using fuzzy based analytic hierarchy approach, Expert Systems With Applications, 35 (2008), pp. 1430-1443

[8] De-li, Z.: Research on bearing capacity identification of long-span Bridges, Bridge construction, 48 (2018) 5, pp. 43-47

[9] Ning-Bo, W., Wei, S., Chuanrui, G., Hua-Ping, W.: Moving load test-based rapid bridge capacity evaluation through actual influence line, Engineering Structures, 252 (2022), pp. 113630

[10] Xue, M.S., Yi, T.H., Qu, C.X., et al.: Structural modal flexibility identification through a novel mode selection method, Journal of Engineering Mechanics, 147 (2021) 3, pp. 06021001

[11] Maas, S., Nguyen, V.H., Kebig, T., et al.: Comparison of different excitation and data sam pling-methods in structural health monitoring, Civil Engineering Design, 1(2019), pp. 10-16

[12] Yun, Z., Wei-jian, Y., Yun-zhong, J., Li-min, X., Mister, L.: China journal of highway and transport, 28 (2015) 9, pp. 46-56

[13] Yun, Z., Yun-zhong, J., Wei-jian, Y., Li-min, X., Fanding, J.: Experimental research on structural damage diagnosis based on modal flexibility theory, Journal of Hunan University (Natural Science), 42 (2015) 5, pp. 36-45

[14] Tian, Y.D., Zhang, J., Xia, Q., et al.: Flexibility identification and deflection prediction of a three-span concrete box girder bridge using impacting test data, Engineering Structures, 146 (2017), pp. 158-169

[15] Tian, Y.D., Zhang, J., Han, Y. X.: Structural scaling factor identification from output-only data by a moving mass technique, Mechanical Systems and Signal Processing, 115 (2019), pp. 45-49

[16] Necati Catbas, F., Brown, D.L., Emin Aktan, A.: Use of modal flexibility for damage detection and condition assessment: Case studies and demonstrations on large structures, Journal of Structural Engineering, 132 (2006) 11, pp. 1699-1712

[17] Shuang-lin, G.: Identification method of displacement compliance and strain compliance based on impact vibration, Southeast University, 2015.

[18] Yong-ding, T.: Identification and performance evaluation of bridge structural flexibility based on environmental vibration, Southeast University, 2016.

[19] JTG/T J21-01-2015: Load test methods for highway bridge, https://www.chinesestandard.net/PDF/English.aspx/JTGTJ21-01-2015, [1.6.2023.]

[20] JTG/T J21-2011: Specification for inspection and evaluation of load-bearing capacity of highway bridges, https://www.chinesestandard.net/PDF/English.aspx/JTGTJ21-2011, [1.6.2023.]

[21] CJJ/T 233-2015: Technical code for test and evaluation of city bridges, https://www.chinesestandard.net/PDF/English.aspx/CJJT233-2015, [1.6.2023.]

[22] Yong-gao, C., Zhen-yu, Z.: Modal parameter identification of bridge structure based on improved EEMD algorithm, Journal of highway and transportation science and technology, 35 (2018) 4, pp. 49-57

[23] Ze-xin, C., Yong, H., Zhen-yu, Y., et al.: Earthquake engineering and engineering vibration, 39 (2019) 2, pp. 213-224

[24] Qi-cheng, R.: Research on bridge rapid diagnosis technology based on compliance coefficient, Civil Aviation University of China, 2018.

[25] Buhmann, M.D.: Radial basis functions: Theory and implementations, Cambridge University Press, New York, 2003.

[26] Morlier, J., Chermain, B., Gourinat, Y.: Original statistical approach for the reliability in modal parameters estimation, 27th International Modal Analysis Conference, Orlando, 2009.

[27] Shepard, D.: A two-dimensional interpolation function for irregularly - spaced data, 23rd ACM National Conference, New York, 1962., pp. 517-524

[28] Xing-jun, Q., Yue,Z., Qi, Z.: Numerical method for static load test of skew bridge based on modal deflection, Journal of building science and engineering, 37 (2020) 3, pp. 55-62

[29] Qi, X.: Rapid test method and theoretical innovation of bridge based on impact vibration, Southeast University, 2017.